

MAIN MAGNET AND CENTRAL REGION DESIGN FOR A 10 MEV PET CYCLOTRON CYCHU-10*

B. Qin [#], J. Yang, K. Liu, D. Li, L. Zhao, T. Yu, Y. Xiong, M. Fan
Huazhong University of Science and Technology, Wuhan, 430074, P. R. China.

Abstract

Low energy compact cyclotrons for short-life isotopes production delivered to the Positron Emission Tomography (PET) facilities have foreseeable prospects with growing demands in medical applications. The Huazhong University of Science and Technology (HUST) proposed to develop a 10MeV PET cyclotron CYCHU-10. The design study of the main magnet and the central region was introduced. A matrix shaping method with the radial fringe field effect and artificial control was adopted to obtain field isochronisms precisely. The central region was optimized to attain 35°RF phase acceptance and low vertical beam loss rate.

INTRODUCTION

Commercial cyclotrons for isotopes production have a dramatic increase since 1990s, with the energy ranging from 5MeV to 30MeV [1]. The majority cyclotrons of this type were employed for short-life isotopes production in PET facilities. Recent years, PET and PET-CT were installed in some hospitals in China with upward trend, which shows considerable demands for low energy compact cyclotrons. HUST proposed to build a compact cyclotron CYCHU-10 to extract 10MeV protons, which is designed for short-life isotopes production in PET system. For the sake of compactness and robust, CYCHU-10 adopt internal cold-cathode PIG ion source. The main isotopes produced by this machine will be ¹¹C, ¹⁵O and ¹⁸F.

Table 1: Main Parameters of CYCHU-10

Parameter	Value
Beam species	Negative hydrogen
Ion source	Cold-cathode PIG source
Maximum beam energy	10 MeV
Beam current	40 μA
Sector numbers	4
Sector open angle	48° ~ 53°
Hill / valley gap size	2.4 cm / 9.6 cm
Central magnetic field	1.63 T
Radio frequency	99.2 MHz
Dee voltage	34 kV

*Work supported by National Nature Science Foundation of China (10435030) and National Science Foundation for Post-doctoral Scientists of China (20080430973)

[#] bin.qin@mail.hust.edu.cn

Some design works concerning the magnet and the resonance cavity have been performed to confirm main parameters [2, 3], as shown table 1.

Compared with the common used ‘deep valley’ magnet structure, we choose another scheme with narrow valley gap about 10 cm. It enhanced the average magnetic field and made the total magnet more compact. But due to the small gap scale between the hill/valley, the field flutter is moderate, which decreases the axial focusing of the beam. The structure need to be optimized to compensate this effect. Meantime, the coupling of the magnet geometry and the resonance cavity becomes extremely important.

MAGNET DESIGN AND SHAPING

The basic parameters of the magnet, such as the pole radius and the gap size are determined by approximate analytical method and 2D calculation. Then the parameterized 3D magnet model is created by Opera-3D/TOSCA, see Fig. 1.

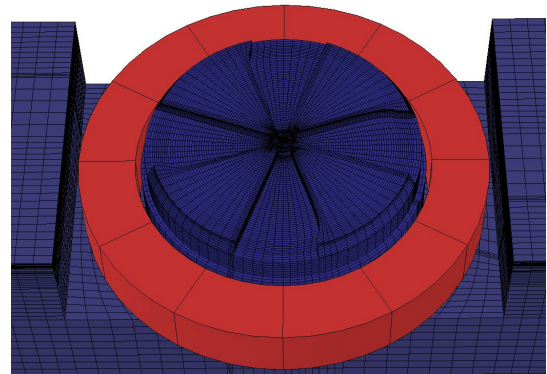


Figure 1: Magnet model of CYCHU-10

The initial magnetic field is calculated by TOSCA. For calculation efficiency, the 90 degree model with 160,000 quadratic hexahedra elements was used. The maximum hill and valley field is about 2.1T and 1.0 T. We use PTP [4] code to perform equilibrium orbit analysis by direct integration method.

The magnetic field optimization for the isochronisms and focusing performance is an iterative process with the aid of the equilibrium orbit calculation. The particle cyclic frequency $f_p(r)$ can be calculated by integration of motion equations accurately, and then the isochronous field error is evaluated by Equ. (1).

$$\Delta B(r) = B_{\text{iso}}(r) \cdot \gamma^2(r) \cdot (f_p(r) - f_0) / f \quad (1)$$

During the magnet pole shaping process of compact cyclotrons, there are different ways to transform the field error to the geometric changes of the magnet pole, or in

Magnets

T09 - Room Temperature Magnets

regular form: the pole angle. Here we compared two methods: 1) the linear hard-edge model; 2) the matrix method that include the nonlinear radial fringe field effect.

Hard Edge Model

The hard edge model is an approximate method to describe the azimuthal magnetic field. The relative method has been discussed in [4], and the sector pole angle change $\Delta\eta(r)$ is calculated by Equ. (2), where $B_H(r)$, $B_V(r)$ are the hill and valley magnetic field, and N is the sector number.

$$\Delta\eta(r) \approx \Delta B(r) \cdot (2\pi/N) \cdot (B_H(r) - B_V(r)) \quad (2)$$

In general, a pole angle change list $\{\Delta\eta(r_1), \dots, \Delta\eta(r_n)\}$ is calculated and imported into the revised magnet model for iterative isochronous field optimization.

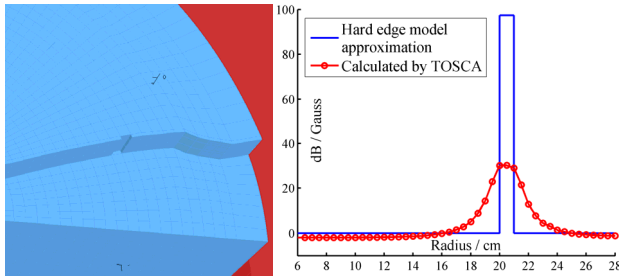


Figure 2: Compare of the hard edge approximation and the realistic field change for a cutting block.

One problem of the hard edge model is that it ignores the radial fringe effect as shown in Fig. 2. We cut one block with 3mm thickness and 10mm radial size from the pole and observe the average magnetic field difference. It's a pulse for the hard-edge approximation with the peak $\Delta B = 97.4\text{Gs}$. While from the realistic calculation, the peak value $\Delta B = 34.0\text{Gs}$ is only 1/3 compared with the hard-edge approximation. But the two integrals $\int \Delta B_{H-E} \cdot dl = 97.4\text{Gs} \cdot \text{cm}$ and $\int \Delta B_{\text{real}} \cdot dl = 96.3\text{Gs} \cdot \text{cm}$ have a good coincidence, which can be explained as the radial fringe effect of a cutting block.

It's obvious that the prediction of the hard-edge model is not accurate: 1) the peak value is far less than the approximation; 2) the nonlinear radial fringe effect takes extra shimming effect. This method will take more iterations to achieve convergence of field isochronism.

Matrix Method with Radial Fringe Field Effect

The shimming process can be accurately controlled by a sequence of cutting thickness at various radius with two assumptions: 1) the magnetic field change is proportional to the cutting area; 2) the total shimming effect is the superposition of independent cutting along radius [5].

The first assumption can be easily proved by the hard-edge model in previous section, and the second one is true when the cutting size is small relatively, which has been validated by TOSCA simulations. So it is possible to give an accurate prediction for the pole shape change

Magnets

T09 - Room Temperature Magnets

according to the required isochronous field, with the pre-calculated radial fringe effect data and linear combination of the shimming thickness at different radius.

The average radial magnetic field change vector \mathbf{y} can be represented as the multiple linear regression model:

$$\mathbf{y} = \mathbf{X} \cdot \boldsymbol{\beta} + \boldsymbol{\varepsilon} \quad (3)$$

Where $\boldsymbol{\beta}$ represents shimming vector, \mathbf{X} is the correlation matrix which can be pre-calculated while cutting unit shimming block at different radius, and $\boldsymbol{\varepsilon}$ is the vector of random disturbances.

The least squares solution of Equ. (3) is $\bar{\boldsymbol{\beta}} = (\mathbf{X}' \cdot \mathbf{X})^{-1} \mathbf{X}' \cdot \mathbf{y}$, which gives a quick reference for the pole shimming, but in most situation, the inherent oscillation caused by the multiple linear regression is unacceptable for magnet shaping both in the design process and the machining process. So it is necessary to determine the final shimming value with artificial control.

We developed a software tool using Matlab to predict and control the shimming value according to the equilibrium orbit analysis result, as shown in Fig. 3. The initial shimming combination is estimated by multiple linear regression, and then each shimming value can be adjusted separately. If the improved shimming vector is $\boldsymbol{\beta}_{\text{imp}}$, then the final shimming effect is calculated by $\mathbf{X} \cdot \boldsymbol{\beta}_{\text{imp}}$. This artificial control provides an accurate and stable method to control the shimming process.

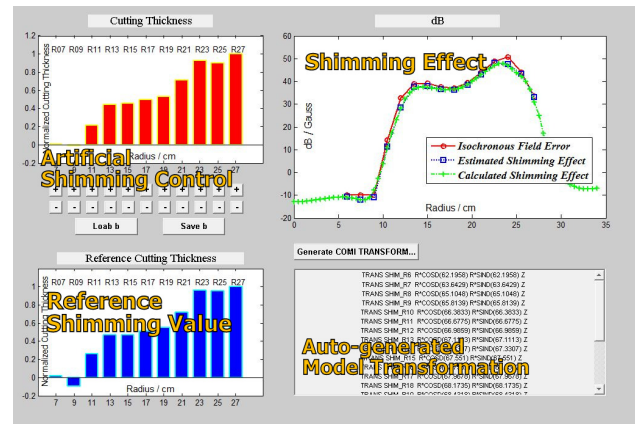


Figure 3: User interface magnet shimming

The shimming effects of two methods are compared for a given isochronous field error profile in Fig. 4. As can be seen, the TOSCA calculated shimming effect using the matrix method is very close to the predicted result. But the shimming effect using the hard-edge model has considerable discrepancy to the desired values. In this example, the convergence of field isochronism is rapid when using the matrix method, and after one iteration, the frequency error can be controlled within 0.05%.

Fig. 5 shows the tune shift during acceleration. It was optimized by adjusting the magnet structure to avoid integer tune crossing at extraction region.

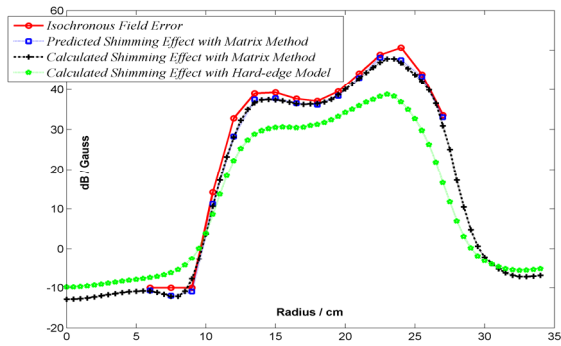


Figure 4: Compare of the shimming effect of two methods

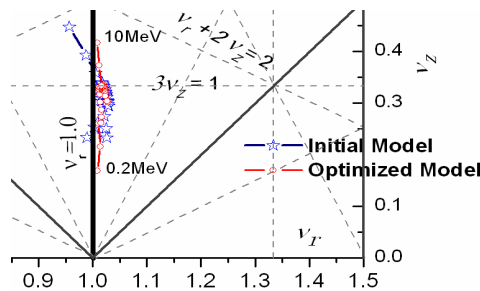


Figure 5: Tune diagram from 0.2MeV to 10MeV.

CENTRAL REGION DESIGN

A cold-cathode PIG source was adopted for internal beam injection in CYCHU-10. Fig. 6 shows the magnet and dee structure. To compensate weak field flutter and increase axial focusing in the central region, the magnet pole is shaped with an elliptic curve fitting on axial dimension for maintaining the smooth negative magnetic field gradient. Then the dee and dummy dees are adjusted to match with the magnetic field.

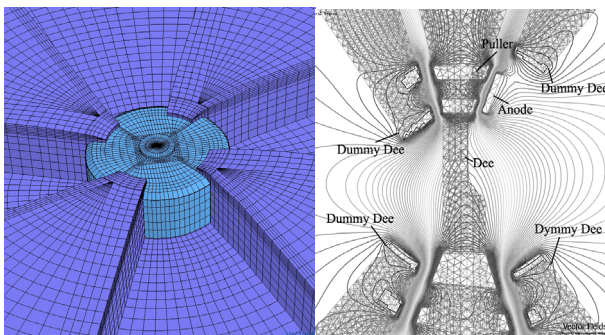
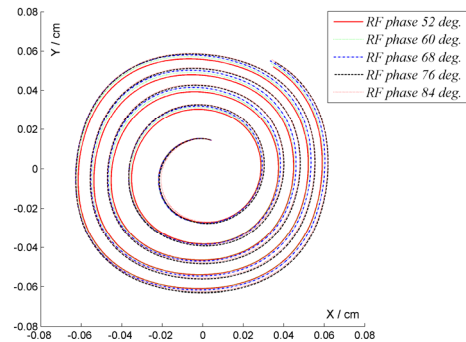


Figure 6. The central magnet and dee structure

We developed a code to calculate beam trajectories, centering and energy gain with direct Runge-kutta integration of particle motion in combined electrical and magnetic field maps. A method using OPERA3D built-in function was employed for code test [6]. A good matching of results was achieved, and the difference of trajectories in the mid-plane is lower than 0.8%.

Fig. 7 shows beam trajectories with 32° RF phase width. The radial and axial RF phase acceptance is about 35 degrees. The optimized parameter of the ion source slit size $\Delta R \times \Delta Z = 0.8\text{mm} \times 5\text{mm}$ was determined by beam loss study with multi-particle tracing. The simulated vertical beam loss in this condition is less than 4%.

Figure 7: Beam trajectories of first 5 turns with 32° RF phase width

PROGRESS AND FUTURE PLANS

The design and construction of the Cartesian field mapping system was accomplished and introduced in [7]. The granite foundation has a good stabilization to the temperature variation. The position precision can be achieved $\pm 5\mu\text{m}$ both in X and Y direction by servo motors and optical linear encoder systems.

The high quality steel DT8 was purchased from Taiyuan Iron & Steel Company Ltd (TISCO), with very low carbon content less than 0.02%. The forging process of the steel has been completed, and the machining was started. The first magnetic field mapping is expected in 2009 July.

REFERENCES

- [1] Y. Jongen. "Review of Compact Commercial Accelerator Products and Applications". PAC' 1997, Vancouver, May 1997, pp. 3770-3774.
- [2] B. Qin et al. "Small Valley Gap Magnet Design for a 10MeV PET Cyclotron". ICEMS 2008, Wuhan, Oct. 2008, pp. 906-909.
- [3] L. Cao et al. "Preliminary Design of RF Cavities for the Cyclotron CYCHU-10", these proceedings.
- [4] B. Qin et al. "Design study of compact cyclotron magnet in virtual prototyping environment," PAC' 2007, Albuquerque, June 2007, pp. 3354-3356.
- [5] W. Cleeven et al. Magnetic Field Calculation and Shimming of the Self-extraction Cyclotron. CYCLOTRONS' 2001, pp. 348-350.
- [6] D. Campo, private communication, 2008
- [7] J. Yang et al. "Magnetic Field Measurement System for CYCHU-10", these proceedings